Proceedings of the 21st ICSMGE, Vienna, Austria, 14 – 19 June 2026. Pistrol, Adam & Schweiger (eds.)
Published by: ÖGG, Austrian Society for Geomechanics, Salzburg, Austria, ISBN 978-3-9503898-4-5
https://doi.org/10.53243/ICSMGE2026-260

Development of a model for the prediction of the bearing capacity of ductile driven piles from pile driving time

Juan Corazza, Oliver Reul
Department of Geotechnical Engineering, University of Kassel, Germany, j.corazza@uni-kassel.de

Johannes Berndt
Henne + Berndt Geotechnik Ingenieure GmbH, Germany

Bernhard Schrötter
TRM Tiroler Rohre GmbH, Austria

ABSTRACT: Ductile driven piles consist of ductile, spun cast iron pipe segments which are driven into the ground with a hydraulic breaker used as a hammer, completely displacing the surrounding soil material. In the case of piles with shaft grouting, fine-grained concrete or cement mortar is permanently pumped through the inside of the pipe during driving. With over thirty years of development, ductile driven piles represent a valuable solution for deep foundations in terms of space requirement, low vibration and installation speed. In the first phase of a research project, correlations between pile shaft friction and unit pile base resistance, respectively, and the penetration resistance of different sounding methods were established based on the stochastic analysis of an extensive database of pile load tests on grouted ductile driven piles. Moreover, these investigations also indicated a correlation between pile bearing capacity and pile driving time, i. e. the time needed for the pile to be driven with a given equipment. The current second phase of the research project aims to develop a robust model for the prediction of the bearing capacity of ductile driven piles from the pile driving time and the energy actually transmitted to the pile. In the scope of this paper, first results of the investigations on the impact force and energy transmission of hydraulic breakers to ductile driven piles are discussed.

KEYWORDS: ductile driven pile, bearing capacity, driving time, hydraulic breaker, energy measurement

1 INTRODUCTION

Prefabricated driven cast-iron piles (in the remainder of this paper simply referred to as ductile driven piles) have been used for several decades to provide solutions for a wide range of foundation tasks. Ductile driven piles are driven into the ground with a hydraulic breaker used as a hammer, completely displacing the surrounding soil.

A widespread method of estimating the bearing capacity of driven piles is the use of some form of pile driving formula, relating the measured permanent displacement (or set) of the pile at each blow of the hammer, to the bearing capacity (Fleming, et al., 2009). However, driving formulae (e.g. Hiley, 1925, Gates, 1957) usually require the dynamic ram energy from the driving system to the pile as an input, which according to (Fleming, et al., 2009) is one of the largest sources of error. For ductile driven piles the measurement of the actually transmitted energy is a specially challenging task due to the use of high frequency hydraulic breakers as a driving hammer. Therefore, often simple approaches which correlate the time required to install the pile, i.e. the driving time, to the bearing capacity of the ductile driven pile are applied in practice.

More sophisticated approaches may be used to assess the pile bearing capacity when stress wave data is obtained in dynamic load tests. Frequently, these models are based on the numerical solution for unidimensional wave propagation proposed originally by Smith (1960), which over the years has been improved by different researchers (e.g. Holeyman, 1985, Randolph and Simons, 1986 and Salgado, et al., 2015).

A current research project focuses on the development of a model for prediction of the bearing capacity of ductile driven piles which considers the driving time and the energy actually transmitted to the pile. In the scope of this paper, first results of the investigations on the impact force and energy transmission of hydraulic breakers to ductile driven piles are discussed. Furthermore, a correlation between driving time and pile bearing capacity is presented which is based on the evaluation of a database containing results of load tests on ductile driven piles.

2 DUCTILE DRIVEN PILES

2.1 *Pile system*

Ductile driven piles consist of ductile, spun cast iron pipe segments which are driven into the ground with a hydraulic breaker used as a hammer, completely displacing the surrounding soil material. The required pile length can be reached through the assembly of various pipe segments by means of spigot and socket joints. The first pipe segment is placed in the so-called pile shoe, which has the same diameter as the pipe in the case of a pile without shaft grouting and a larger diameter in the case of a pile with shaft grouting (Figure 1).

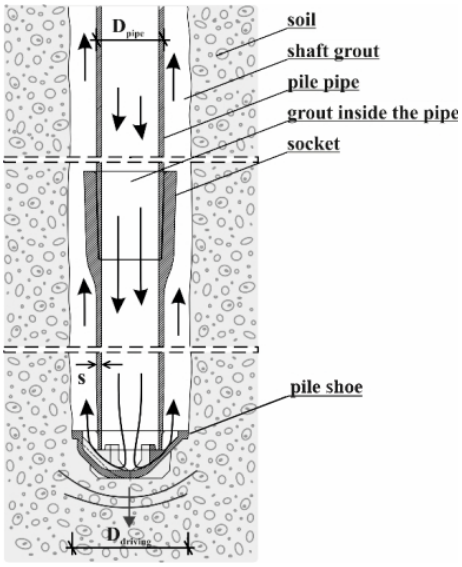

Figure 1. Ductile driven pile with shaft grouting.

Table 1. Dimensional properties of ductile iron pipes

Pipe type	Pipe diameter D_{pipe} [mm]	Wall thickness s [mm]			
Type 98	98	6,0	7,5		
Type 118	118	7,5	9,0	10,6	
Type 170	170	7,5	9,0	10,6	13,0

Piles without shaft grouting are mainly end-bearing piles which require a solid soil layer at pile base level. In the case of piles with shaft grouting, fine-grained concrete or cement mortar (hereinafter simply referred to as grout) is simultaneously pumped through the inside of the pipe during driving. The injection grout fills the annular space formed by the oversized pile shoe from the pile base to the pile head. On condition that the soil surrounding the grouted shaft has sufficient strength, piles with shaft grouting are able to transfer a substantial part of the load to the soil by mobilising the shaft friction.

The German national technical approval Z.34.25-230 (DIBt, 2022) contains the nominal dimensions of the pile pipes, which are listed in Table 1.The diameter of the pile shoe $D_{driving}$ must be large enough to create a grout coverage of at least 20 mm in the area of the joints. Depending on the pipe diameter D_{pipe}, pipe thickness s and grout quality (C20/25 or C25/30), the design value of the internal (structural) compressive load capacity varies between $R_{i,d}$ = 450 kN (D_{pipe} = 98 mm; s = 6 mm; without shaft grouting) and $R_{i,d}$ = 2137 kN (D_{pipe} = 170 mm; s = 13 mm; with shaft grouting) according to Z.34.25-230 (DIBt, 2022). Although the thickness of grout cover at the pile shaft is not considered in the calculation of the structural capacity, for piles without shaft grouting a reduced outer diameter is taken into account because of rusting.

2.2 *Driving equipment*

For the installation of ductile driven piles, the only equipment required is an excavator with a suitable hydraulic breaker. The recommendations on piling (DGGT, 2025) suggest an impact frequency between 300 blows/min and 400 blows/min. This impact frequency, termed “Long stroke” as compared to the “Short stroke” mode of the hydraulic breaker which corresponds to 600 blows/min and more, is obviously much higher than for hammers typically used for pile driving. Additionally, it is challenging to maintain the hydraulic breaker in vertical position during the entire driving process to guarantee a constantly perpendicular impact. For these reasons, the determination of a settlement per blow is virtually impossible to record under the conditions of a construction site without specialized equipment with a high sampling rate. As an alternative, the driving time is widely used as a driving criterion in construction practice.

As the working principle of hydraulic breakers differs considerably from that of the hammers typically used for pile driving, no comprehensive modelling of the driving process of ductile driven piles has been carried out to date. In order to develop a model to simulate driving of ductile driven piles, a thorough understanding of the influence of the working conditions of the equipment is essential. The energy transmitted into the ductile driven pile represents one of the most important factors influencing the driving process. With otherwise identical boundary conditions, e.g. soil stratification and properties, pile pipe cross-section and length, it can be assumed that a higher energy input leads to a decrease in the driving time. Careful assessment of the energy input is therefore of fundamental importance for identifying a correlation between driving time and pile bearing capacity.

The relevance of the operating parameters of the excavator and hydraulic breaker for the efficient energy transmission to the pile as well as for the overall quality of the driving process is already known from construction practice (Hayden, et al., 2022). The main operating parameters of the hydraulic breaker, which have a significant influence on its power and energy output, are briefly introduced below.

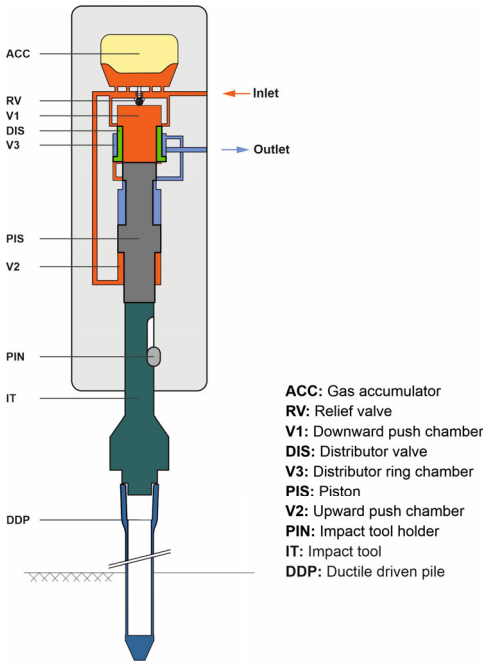

Figure 2. Schematic drawing of a hydraulic breaker, adapted from (Giuffrida and Laforgia, 2005).

The working principle of hydraulic breakers generally consists of the oscillation of a piston caused by the reciprocating motion of a distributor. The working cycle will be explained through the schematic drawing of the device in Figure 2, adapted from Giuffrida and Laforgia (2005). Immediately after a blow, when the piston (PIS) is in its lowest position and allows the flow of oil at the operating pressure to the ring chamber of the distributor (V3), the distributor (DIS), represented here as a sleeve valve, starts to lift. The distributor (DIS) in its upward movement then switches the connection of the downward push chamber (V1) from the inlet to the outlet, allowing for its rapid drainage. In the upward push chamber (V2) there is always oil at the operating pressure, which pushes the piston (PIS) upwards and connects V3 to the outlet. The resulting drainage of V3 allows the distributor (DIS) to move downwards. The connection of V1 to the inlet is then opened again and oil flows in, both from the inlet and the gas accumulator (ACC), to push the piston (PIS) downwards producing a blow against the impact tool (IT).

In order to record reliable data during the driving of ductile driven piles, the following parameters and settings of the driving equipment require special attention:

- The oil flowrate determines how fast the working cycle described above takes place and thus influences the impact frequency.
- The oil pressure defines the magnitude of the forces that push the piston both upwards and downwards. It is dependent of the flowrate of the oil pumped from the excavator and the losses in the hydraulic circuit before the inlet. An insufficient pressure will lead to a lower impact force, and in extreme cases may not be strong enough to set the piston in motion.
- The nitrogen pressure in the gas accumulator influences the behaviour of the hammer during impact. An insufficient gas pressure could lead to reduced flow into V1 and consequently to a lower downward velocity of the piston.

On the other hand, with an excessive gas pressure the accumulator cannot store sufficient oil to push the piston downwards.

Further discussions on aspects of quality management during the installation of ductile driven piles can be found in Hayden et al. (2022) and Kriechbaumer, et al. (2025).

2.3 *Data base for ductile driven piles*

To investigate the bearing behaviour of ductile driven piles, available data on pile load tests were collected resulting in a database containing 387 pile load records from 121 different projects (Berndt, 2022). As part of this process, additional pile load tests applying various static and dynamic testing methods were performed on ductile driven piles in clayey soil (Berndt, et al., 2019) and sandy soil (Berndt, et al., 2021).

A data sheet was first created for each test pile, containing both general project information and information specific for the test pile. The methods used for site investigation were also documented. Sounding profiles were then digitized so that sounding resistances, such as e.g. the CPT cone resistance q_c, are available in digital form continuously along the pile shaft. Additionally, soil layer boundaries for the respective pile location were derived from the geotechnical reports and the soils were classified into cohesive/non-cohesive layers. Table 2 provides information on project data contained in the database.

Table 2. Data sets classified according to the methods of sounding and pile load testing (Berndt, 2022).

Sounding	Total number	Dynamic	Static		
			compression	tension	bi-directional
CPT	58	12	28	6	12
DPH	130	53	51	9	17
DPSH	44	43	1	0	0
SPT	113	40	63	10	0
Others	42	21	15	6	0
Σ	387	169	158	31	29

CPT Cone Penetration Test
DPH Dynamic Probing; hammer mass: 40 kg ≤ m < 60 kg
DPSH Dynamic Probing; hammer mass: m > 60 kg
SPT Standard Penetration Test

Table 3. Empirical data ranges for $q_{s,k}$ and $q_{b,k}$ for shaft-grouted ductile driven piles in non-cohesive soils (Berndt, 2022).

q_c [MN/m²]	$q_{s,k}$ [kN/m²]	$q_{b,k}(s_{ult})$ [kN/m²]
7,5	135 to 165	3300 to 3900
15,0	195 to 230	4600 to 5500
≥ 25,0	250 to 300	6000 to 7100

q_c CPT cone resistance
s_{ult} = 0.1·D_p

Table 4. Empirical data ranges for $q_{s,k}$ and $q_{b,k}$ for shaft-grouted ductile driven piles in cohesive soils (Berndt, 2022).

s_u [kN/m²]	$q_{s,k}$ [kN/m²]	$q_{b,k}(s_{ult})$ [kN/m²]
60*1/100*2	45 to 55	1300 to 1500
150	75 to 85	1600 to 1900
≥ 250	95 to 110	2000 to 2400

2.4 *Empirical values for the prediction of the ultimate axial capacity of ductile driven piles*

On the basis of the static pile loads test documented in the pile database, Berndt (2022) carried out investigations on the ultimate axial capacity of ductile driven piles using a multi-linear regression model (e.g. Hartung, et al., 2009). In line with the framework of the German Recommendations on Piling (DGGT, 2025), empirical values were derived for the pile shaft friction and the pile base resistance per unit area depending on the CPT cone resistance q_c and the undrained shear strength s_u, respectively (Berndt, et al., 2023).

Table 3 and Table 4 show the bandwidths of the characteristic shaft friction $q_{s,k}$ and the pile base resistance per unit area $q_{b,k}$ in the form of the 10% quantile and the 50% quantile for non-cohesive and cohesive soils, where $q_{b,k}(s_{ult})$ corresponds to a settlement equal to 10% of the pile diameter D_p.

3 CORRELATION BETWEEN DRIVING TIME AND BEARING CAPACITY

Based on the evaluation of the database (section 2.3), a first approach for a correlation between pile driving time and the bearing capacity of ductile driven piles was proposed by (Berndt, 2022).

As the actual correlation between these variables is unknown, the root functions in Equations (1) to (2) were chosen to approximate a nonlinear relationship. The coefficients a_c and a_{nc} and b_c and b_{nc} summarized in Table 5 define shaft friction and base resistance per unit area of grouted ductile driven piles and were determined for cohesive and non-cohesive soils, respectively.

$$q_s = \sqrt{DT_i} \cdot a \quad (1)$$

$$q_b = \sqrt{DT_{base}} \cdot b \quad (2)$$

where $q_{s,c,i}$, $q_{s,nc,i}$ = shaft friction in a cohesive and non-cohesive soil layer i, respectively; $q_{b,c}$, $q_{b,nc}$ = base resistance per unit area in cohesive and non-cohesive soil, respectively; a_c, a_{nc} = coefficient of shaft friction in cohesive and non-cohesive soil, respectively; b_c, b_{nc} = coefficient of base resistance per unit area in cohesive and non-cohesive soil, respectively; DT_{base} = driving time of the last 10 cm related to the pile base area A_{base}; $DT_{shaft,i}$ = driving time in layer i related to the pile base area A_{base}.

Table 5. Coefficients for the correlation between driving time and bearing capacity (Berndt, 2022).

Shaft friction		Base resistance per unit area	
a_c	a_{nc}	b_c	b_{nc}
3,5	6,5	22,0	36,0

Figure 3a compares the measured bearing capacity R_m with the bearing capacity R_{cal} calculated with the approach described above for the n = 69 pile tests where reliable driving time recordings were available. The histogram in Figure 3b shows the frequency distribution of the relative difference GR between calculated and measured bearing capacity, expressed by Equation (3).

$$GR = \frac{|R_m - R_{cal}|}{R_m} \quad (3)$$

Although it was initially assumed that numerous disturbance factors such as the experience of the equipment operator or the manual recording of time and penetration would negatively influence the quality of the regression, the investigation revealed a comparatively high correlation with adj. R^2 = 0.65 (incl. outliers) (Berndt, 2022).

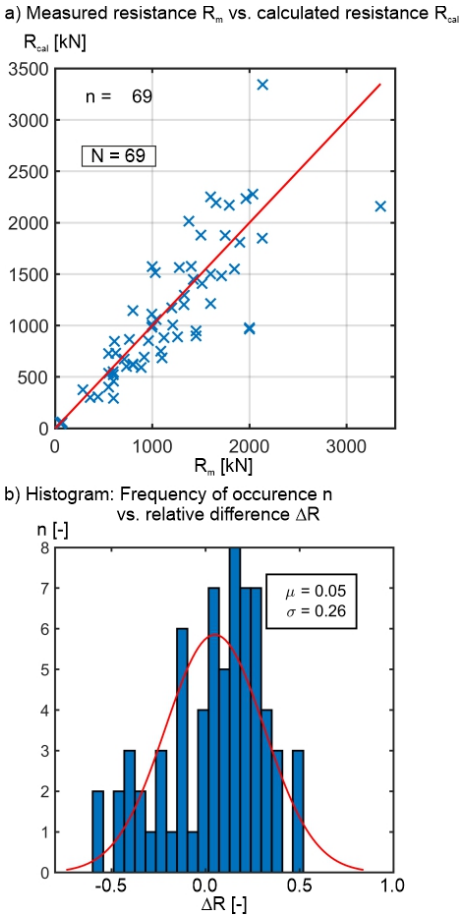

Figure 3. Correlation between total load capacity and driving time (DTx) (Berndt, 2022).

4 CURRENT TESTING PROGRAM

4.1 *Overview*

In the scope of the current research project the influence of the driving process on the subsequent bearing behaviour of ductile driven piles is to be investigated with the aim to develop a prediction model of the pile bearing capacity of ductile driven piles which considers the driving time and the energy actually transmitted to the pile. In order to achieve this goal, the following test stages are planned, some of which overlap:

Stage A

- Optimization of measurement devices to sustain the comparably high impact frequency.
- Identification of appropriate settings of the hydraulic breaker which allow for defined and controlled energy transmission to the pile.

Stage B

- Measurement of energy transmission to the pile during the driving process on a test site.
- Development of a correlation between the settings of the hydraulic breaker (oil flowrate, oil pressure and nitrogen pressure in the ACC.) and the energy input to the pile
- Evaluation of changes in the soil conditions in the vicinity of the pile due to the driving process.
- Measurement of driving time by means of quality control systems.

Stage C

- Detailed geotechnical investigation of a test site with predominantly non-cohesive soil.
- Installation of grouted ductile driven piles with appropriate settings of the hydraulic breaker:
  measurement of energy transmission during driving for selected piles; detailed recording of the driving time.
- Static and dynamic pile testing of the grouted ductile driven piles to identify ultimate shaft friction and base resistance per unit area.

The following section presents initial results achieved in two field tests during Stages A and B, the full evaluation of which remained in progress at the date of preparation of this paper.

4.2 *Set-up of the field tests*

During the Stages A and B in March 2023 and May 2025 field tests were carried out in Hart im Zillertal, Austria and Illertissen, Germany, respectively. The subsoil at the test sites comprised silty gravel (Zillertal) and gravelly sand (Illertissen).

For the tests in Zillertal an EPIROC MB1650 breaker mounted on a KOMATSU PC210 excavator was used as a driving hammer. Five pile pipes (D_{pipe} = 118 mm; s = 9.0 mm) with pile shoes for ungrouted piles ($D_{driving}$ = 118 mm) were driven in the ground until they stood on a previously buried block of granite at a depth of 3,50 m which simulated a rigid layer.

In Illertissen the driving equipment consisted of an EPIROC HB2000 breaker mounted on a LIEBHERR R924 excavator. Two pile pipes (D_{pipe} = 118 mm; s = 10.6 mm) were driven to a depth of 3,50 m in the relatively uniform gravelly sandlayer. Despite the use of enlarged pile shoes for grouted piles ($D_{driving}$ = 270 mm), the piles were not grouted during driving.

4.3 *Settings of the hydraulic breaker*

Following the recommendations of the manufacturer (Epiroc, 2025) the target values for the settings of hydraulic breaker documented in Table 6 were defined. Based on these target values the manufacturer of the hydraulic breaker calculated an output energy of $E_{output,breaker}$ = 3450 Nm according to the calibration procedure of the Mounted Breaker Manufacturers Bureau (2001).

In order to maintain controlled driving conditions, the oil and gas pressure as well as the oil flowrate and the temperature were recorded during the test in Zillertal. However, to take direct readings of the operating pressure and flowrate the breaker must be decoupled from the excavator and replaced by a measuring turbine (Figure 4). For this reason, the readings were carried out before and after the driving process.

The measured flowrate showed a reasonable agreement with the target value (Table 6) while for the operating pressure and especially the gas pressure significantly higher values were recorded towards the end of the driving process. This was probably due to the fact that nitrogen was added immediately before the first pile driving, as the gas pressure measurement was too low. However, with an ambient temperature of $T_{ambient} \approx 1$°C at this point the hydraulic breaker was still cold and far away from its typical operating temperature of $T_{operating} \approx 60$°C.

As a consequence, for the test in Illertissen the driving equipment was thoroughly warmed up before the driving of the test piles and only then the gas pressure and operating temperature were measured. Further periodic controls consisted of the measurement of the gas pressure and temperature in the accumulator before and after the driving of each test pile. During the test, the measured values remained well within the target values.

Table 6. Target values for the settings of the hydraulic breakers

Parameter		Target values	
		Zillertal	Illertissen
Operating pressure	MPa	18	18
Oil flow rate	l/min	170	190
Piston accumulator gas pressure	MPa	1,26	1,48
Impact rate	blows/min	300 to 400	320

Figure 4. Test Zillertal: Measurements of oil flowrate before driving.

4.4 *Measurement devices*

The main objective of the measurements is the determination of the input energy in the pile $E_{input,pile}$ for individual blows. Therefore, accelerations and strains at the pile head, i.e. beneath the socket, need to be measured during the driving process to calculate velocities and forces.

For the test in Zillertal the measurement devices comprised two accelerometers and two strain sensors which were attached to the pile pipe with one and two screws each, respectively. The pile pipes were turned in a lathe in the area of the measurement cross-section before the tests (Figure 5a). This was intended to achieve a smooth pipe surface and a defined pipe cross-sectional area (s ≈ 7.8 mm). Additionally, each pile pipe was instrumented with four strain gauges glued directly on the shaft surface (Figure 5b).

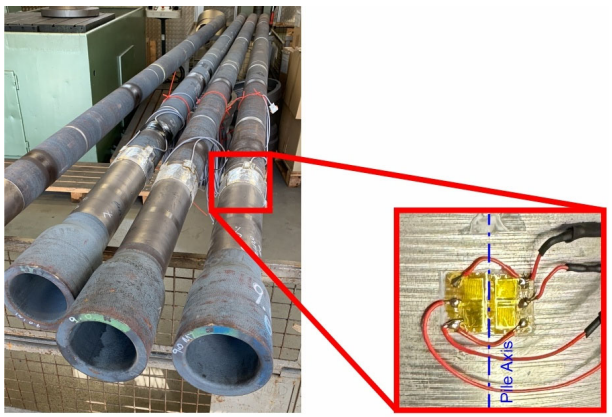

Figure 5. Preparation and instrumentation of test piles.

Figure 6. Test Zillertal: Sheared screw that held an accelerometer.

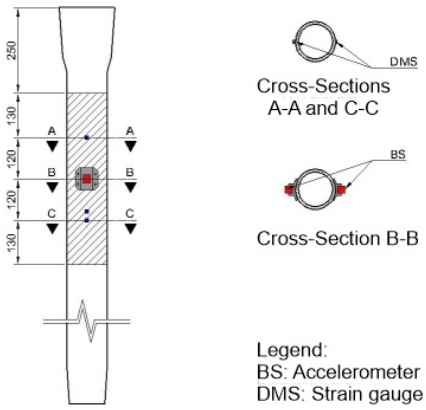

Figure 7. Test Illertissen: Location of accelerometers and strain gauges.

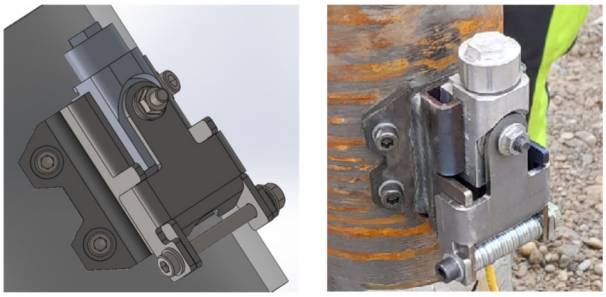

Figure 8. Test Illertissen: Holder for accelerometers.

Though the recorded strains and accelerations lay well between the measuring limits of the measurement devices, the inertia forces sheared the screws (Figure 6) and led to a disassembling of the instruments during the driving process. However, the glued strain gauges remained operative during the entirety of the driving processes and the recorded data could be used with the available acceleration measurements to calculate the input energy in the pile.

For the test in Illertissen the measurement devices attached to each pile pipe comprised two accelerometers and six strain gauges (Figure 7). As for the test in Zillertal, the strain gauges were glued directly on the pile pipes which had been turned in a lathe resulting in a pipe thickness s ≈ 9,8 mm. For the accelerometers a special holder was developed which was attached to the pile pipe with four screws (Figure 8).

In general, the modified set-up of the measuring devices proved successful and enabled the instruments to withstand the exerted loads during the driving process. The presentation and discussion of the measurement data will be the subject of a later publication.

4.5 *Measurement of energy transmission to the pile during the driving process*

From the known values of the cross-sectional area A of the pile and the elasticity modulus E of the cast iron, the input energy $E_{input,pile}$ was derived from the measurements by means of Equation (4):

$$E_{input,pile} = E \cdot A \cdot \int \varepsilon(t) \cdot v(t) \cdot dt \qquad (4)$$

where $\varepsilon(t)$ = measured strain and $v(t)$ = measured velocity.

Whereas the results of the test in Illertissen are still being evaluated as of the date of submission of the present article, the results of the measurements in Zillertal are presented in Figure 9 and in Table 7. It is important to note, that despite the individual results exhibit a relatively small scatter, the average energy

transmitted to each pile from the same hydraulic breaker and under similar subsoil conditions varies by approximately 18%. Uncertainties of the working parameters of the hydraulic breaker such as oil and gas pressure may be a main cause for this variation and need to be investigated in more detail in the future.

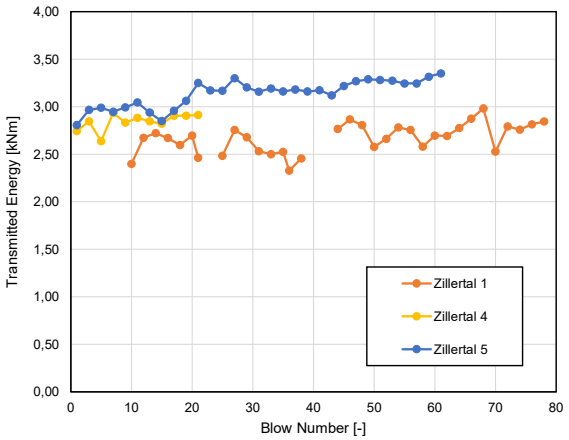

Figure 9. Test Zillertal: Measured input energy of piles driven with a MB1650 breaker.

Table 7. Test Zillertal: Comparison of the output energy of a MB1650 breaker with the measured input energy.

Pile	$E_{output,breaker}$ [J]	$E_{input,pile}$ [J]	Standard deviation [J]
Zillertal 1	3450	2667	150
Zillertal 4	3450	2842	83
Zillertal 5	3450	3137	142

5 CONCLUSIONS

Based on the evaluation of an extensive database on pile load tests on ductile driven piles a first approach for a correlation between pile driving time and the bearing capacity of ductile driven piles was proposed. However, to improve this correlation the energy actually transmitted to the pile during the driving process with a hydraulic breaker used as a hammer needs to be considered.

A first set of field tests carried out to quantify this energy transmission showed the importance of the settings of the hydraulic breaker such as oil flow rate, oil operating pressure and nitrogen pressure in the gas accumulator. During the field test the attachment of measurement accelerometers and strain sensors to the pile pipe by means of screws proved challenging and required the development of special holders. However, preliminary results of the measured input energy are promising and will be further investigated in additional field tests in successive stages of the research project.

The results of the testing program will then provide the base for the development and calibration of a numerical model to simulate the driving process of ductile driven piles with the aim to estimate the bearing capacity of ductile driven piles from the pile driving time and the energy actually transmitted to the pile.

6 ACKNOWLEDGEMENTS

The contribution of Hollaus Bau GmbH, Kurt Motz GmbH, GSP Gesellschaft für Schwingungsuntersuchungen und dynamische Prüfmethoden mbH and Epiroc Construction Tools GmbH in carrying out the field tests and their valuable contributions to the discussion are gratefully acknowledged.

7 REFERENCES

Berndt, J., 2022. *Untersuchungen zum Tragverhalten von Duktil-Rammpfählen.* Schriftenreihe Geotechnik, H.28. Universität Kassel.

Berndt, J., Hundertmark, A.-K., Reul, O. and Tian, Y., 2021. Numerical simulation of driven displacement piles with respect to installation effects on the basis of in-situ test results. In: *Proceedings of the 20th International Conference on Soil Mechanics and Geotechnical Engineering.* Sydney: International Society for Soil Mechanics and Geotechnical Engineering.

Berndt, J., Reul, O. and Marte, R., 2023. Erfahrungswerte zur Prognose der axialen Grenztragfähigkeit von Duktilrammpfählen. *Bautechnik,* 100(12), pp. 751–760.

Berndt, J., Reul, O., Schrötter, B. and Hayden, M., 2019. Investigation of the bearing behaviour of slender driven piles in clay – Comparison of different static and dynamic methods of pile testing. In: H. Sigursteinsson, S. Erlingsson, and B. Bessason. *Proceedings of the XVII European Conference on Soil Mechanics and Geotechnical Engineering (ECSMGE) 2019.* Reykjavik: The Icelandic Geotechnical Society IGS.

Deutsche Gesellschaft für Geotechnik (DGGT), 2025. *EA-Pfähle: Empfehlungen des Arbeitskreises "Pfähle",*3. Auflage. Berlin, Germany: Wilhelm Ernst & Son.

Deutsches Institut für Bautechnik (DIBt), 2022. *Allgemeine Bauaufsichtliche Zulassung Z-34.25-230.* Berlin, Germany: Deutsches Institut für Bautechnik.

Epiroc, 2025. Safety and operating instructions. Construction Tools GmbH.

Fleming, W., Weltman, A. J., Randolph, M. F. and Elson, W. K., 2009. *Piling Engineering,*3rd ed.: Taylor & Francis Group.

Gates, M., 1957. Empirical formula for predicting pile bearing capacity. *Civil Engineering (ASCE),* 27(6), pp. 65–66.

Giuffrida, A. and Laforgia, D., 2005. Modelling and Simulation of a Hydraulic Breaker. *International Journal of Fluid Power,* 6(2), pp. 47–56.

Hartung, J., Elpelt, B. and Klösener, K.-H., 2009. *Statistik: Lehr- und Handbuch der angewandten Statistik; mit zahlreichen durchgerechneten Beispielen,*15., überarb. und wesentlich erw. Aufl. München: Oldenbourg.

Hayden, M., Chalmovsky, J., Kirchmaier, T., Monsberger, C., Neumann, H. and Racansky, V., 2022. Neueste Entwicklungen der Qualitaätssicherung bei der Duktilpfahlherstellung. In: Österreichicscher Ingenieur- und Architekten-Verein. *Österreichische Geotechniktagung.* Vienna, Austria, 19. und 20. April.

Hiley, A., 1925. A rational pile-driving formula and its application in piling practice explained. *Engineering (London),* 119, 657-658, 721.

Holeyman, A., 1985. Dynamic non-linear skin friction of piles. In: *International Symposium on Penetrability and Drivability of Piles.* San Francisco, California, USA.

Kriechbaumer T., Lopez F. and Heiland J., 2025. Digitalisierung der Qualitätssicherung bei der Installation von Duktilrammpfählen. In: *Mitteilungen des Instituts für Geomechanik und Geotechnik Technische Universität Braunschweig (Heft Nr. 119).* Braunschweig, Germany.

Mounted Breaker Manufacturers Bureau, 2001. Measuring Guide for Tool Energy Rating for Hydraulic Breakers. Construction Industry Manufacturers Association.

Randolph, M. F. and Simons, H. A., 1986. An improved soil model for one-dimensional pile driving analysis. In: *3rd International Conference on Numerical Methods in Offshore Piling.* Nantes, France.

Salgado, R., Loukidis, D., Abou-Jaoude, G. and Zhang, Y., 2015. The role of soil stiffness non-linearity in 1D pile driving simulations. *Géotechnique,* 65(3), pp. 169–187.

Smith, E. A. L., 1960. Pile-Driving Analysis by the Wave Equation. *Journal of the Soil Mechanics and Foundations Division,* 86(4), pp. 35–61.